SUPPLEMENTARY INFORMATION:

a) Wax Appearance Temperature (WAT) and Wax Precipitation Curve (WPC) measurements:

WAT and WPC were measured with a differential scanning calorimeter Mettler Toledo DSC1 equipped with a cooling system able to reach low temperatures (-80 °C). The instrument was calibrated by measuring the temperature and the melting heat of pure indium. For each experiment, 10 mg of the sample was loaded into an aluminum crucibles, which was sealed hermetically. During each experimental run, the sample was first heated to 70 °C and then held isothermally for 5 min. A constant cooling rate of 2 °C/min was subsequently applied and data recording started (from 70 °C to -80 °C).

The WPC was computed from the excess heat, which is released during wax precipitation. This cumulative sum of excess heat is related to the amount of wax, that has precipitated from a temperature T_i above the WAT to a temperature T. By integrating the crystallization peak between the initial temperature T_i and the final crystallization temperature T_f, it was possible to calculate the proportion of waxy crystals, $X(T)$%, at a temperature T related to total crystals according to equation (SI.1):

$$X(T) = \frac{\Delta H(T)}{\Delta H_{total}} \times 100 = \frac{\frac{\int_{Ti}^{T} flow\ heat\ dT}{v_r}}{\frac{\int_{Ti}^{Tf} flow\ heat\ dT}{v_r}} \times 100 \quad \text{(SI.1)}$$

Where v_r (°C/s) is the cooling rate applied to the sample.

Then, by knowing the mass of paraffins $m_{paraffins}$ contained in each sample and the total mass of the sample m_{sample}, the proportion of waxy crystals at a temperature T, C_{wax} *(wt. %),* is given by equation (SI.2):

$$C_{wax} = \frac{X(T) \times m_{paraffins}}{m_{sample}} \quad \text{(SI.2)}$$

For crude oil, two crystallization peaks were detected: a minor peak at 32°C and a major peak at 51°C. For the study, the WAT was considered at 51 °C. It can be noticed that between 51 °C and 32 °C the proportion of crystals evolves slowly from 0 % up to 0.9 % and becomes significant only below 32 °C.

b) Density of the liquid phase ρ_L:

Above the WAT, density measurements of the suspending liquid phase were performed with an Anton Paar DMA5000 densitometer. Crude oil densities of the suspending liquid phase ρ_L were obtained for temperatures below the WAT by extrapolating the density as a linear function of temperature ($\rho_L = aT + b$). For the model oil, densities of Hydroseal (solvent) are directly measured as a function of temperature then extrapolated for lower temperatures.

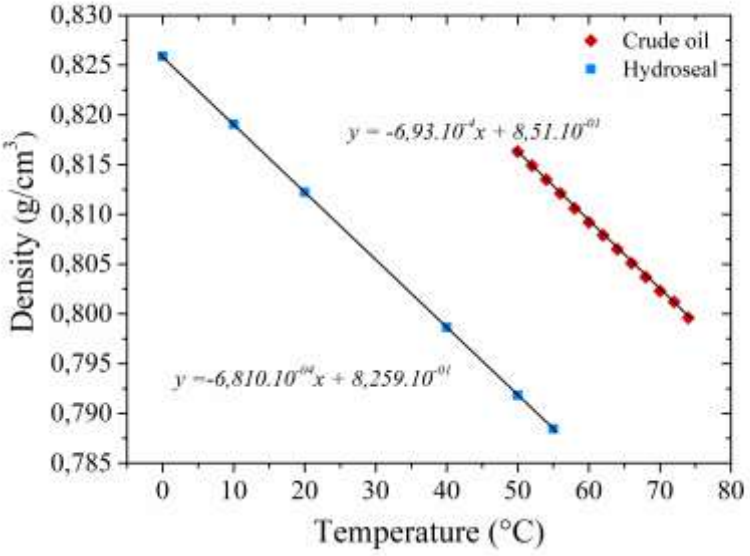

Figure SI-1. *Crude oil and model oil densities as a function of temperature.*

c) The elemental analysis C, H, O, N, S:

The elemental analysis of C, H, O, N, S of the oils was determined by a modified standard method (ASTM D5291) and was used to process the data from SAXS/WAXS. Results can be found in **Table SI-1** and **Table SI-2** below:

Table SI-1. *Chemical properties of the model oil.*

Elements	Model oil
C (wt %)	85.5
H (wt %)	14.53
O (wt %)	0
N (wt %)	0
S (wt %)	0

Table SI-2. *Chemical properties of the crude oil and centrifuged oils (n.d=not determined).*

Elements	Crude oil	Oil 40	Oil 20	Oil 5	Oil 0	Oil -5
C (wt %)	86.2	86.0	85.9	86.0	85.5	85.5
H (wt %)	13.54	13.55	13.47	13.47	13.28	13.19
O (wt %)	0.29	n.d	n.d	n.d	n.d	n.d
N (wt %)	0.13	n.d	n.d	n.d	n.d	n.d
S (wt %)	<0.1	n.d	n.d	n.d	n.d	n.d

d) Calculation of σ and $\bar{n}$ parameters:

$$\bar{n} = \sum_{n_{min}}^{n_{max}} x_n n$$

$$\sigma = \sqrt{\sum_{n_{min}}^{n_{max}} x_n (n - \bar{n})^2}$$

Where x_n is the molar fraction of each C_n and with n_{min} and n_{max} corresponding respectively to the shortest chain and the longest chain in the mixture.

e) Experimental protocol of the temperature-controlled centrifugation:

Temperature-controlled centrifugation experiments have been carried out on the crude oil at five different temperatures: 40 °C, 20 °C, 5 °C, 0 °C and -5 °C. These temperatures are rather easy to control in laboratory conditions. Before starting centrifugation, the waxy crude oil stays in an oven heated up to 70 °C, for one night. After heating, the sample was vigorously stirred to ensure that the entire mixture was a homogenous liquid. Approximately 20 g of the crude oil was then loaded into a centrifuge tube. Then, depending on the desired separation temperature, different cooling techniques were used (thermostatic bath, fridge or air-conditioned lab). Once the centrifuge temperature is reached, the temperature of each tube is kept constant for at least 2 hours before the centrifugation test. The cooled samples were pricked with a spatula to break-up the crystal network formed and release the liquid oil trapped. Then, the centrifugation was performed at the desired temperatures and rotation speeds (18,000 G or 20,000 G) for one night. At the end of the centrifugation, the supernatant liquid oil was collected, taking care not to sample the solid phase which has settled at the bottom of the tube.

f) SAXS Modelling:

The contrast term $\Delta\rho_{scat}$ was obtained from the density and elemental composition (n) of the solvent and particles respectively (supplementary information **b** and **c**). ρ can be written as follow:

$$\rho_{scat} = \frac{1}{V_{cc}}\, b_e \sum_{i}^{N} n_i Z_i \qquad \text{(SI.3)}$$

V_{cc} is the volume considered in the chemical composition, b_e is the scattering length of one electron (b_e = 0.282.10^{-12} cm), Z_i is the atomic number of atom i and n_i the number of atoms of type i in the volume V_{cc}.

For discs or lamellae, a more detailed expression of the form factor for flat discs of total height $2H$ and radius R, in the q domain where $qH \leq 1$ and $qR >> 1$, is given by:

$$P(q) = \frac{2v}{(qR)^2}\, exp\left(-\frac{(qH)^2}{3}\right) \qquad \text{(SI.4)}$$

For dilute systems, if a thickness polydispersity is considered, equation (3) can be rewritten as:

$$I(q) = \Delta\rho_{scat}{}^2 N_p \int_{H_{min}}^{H_{max}} f(H)\, v(H)^2\, P(q,H)\, dH \qquad \text{(SI.5)}$$

Equation (SI.5) is valid in the observed q range, since the interactions between particles are not probed. *f(H)* is the log-normal distribution with σ the variable polydispersity thickness and μ the mean value of the flat disc height:

$$f(H) = \frac{1}{\sigma\sqrt{2\pi}} \exp\left(-\frac{\ln(H/\mu)^2}{2\sigma^2}\right) \qquad \text{(SI.6)}$$

g) WAXS Modelling:

In the WAXS domain, the scattering vector q probes the interatomic distances and the general theory of radio-crystallography apply. Positions of Bragg peaks allow to identify the crystal lattice and the nature of crystalline phase, whereas the peak intensities allow to estimate the phases contents. For orthorhombic unit cells, the following expression relate the Miller index h k l, the interreticular distance of the corresponding family of plan (hkl) d_{hkl} and the unit cell parameters a, b and c.

$$\frac{1}{d_{hkl}^2} = \frac{h^2}{a^2} + \frac{k^2}{b^2} + \frac{l^2}{c^2} \quad \text{(SI.7)}$$

The Scherrer relation is given by :

$$S_{hkl} = \frac{0.89\ \lambda}{\left(\sqrt{FW(S)_{hkl}{}^2 - FW_{instr.}{}^2}\right) cos(\theta_{hkl})} \quad \text{(SI.8)}$$

Where $FW_{instr.}$ stand for the instrumental line broadening. This parameter is usually assessed using the WAXS measurement of a 'perfect' crystal from which the full width at half maximum of a Bragg peak, situated in the same angular range as the sample pic of interest, is extracted. As this instrumental line broadening depends on the detector resolution, the q calibration standards, *i.e* Ag Behenate and LaB_6 respectively for SAXS and WAXS, are also used here to estimate FW_{instr}.

h) Magnetization evolution:

In order to confirm that the removal of the first three points did not affect the measurements, we compared the evolution of the magnetization at the first measured point ($M_{(t=2\tau)measured}$) in the case of the multi-component decomposition and two-component decomposition after removing three magnetization points (**Figure SI-2**). The results show that there is no difference between

the two series of measurements. This procedure allowed us to focus only on the two protons populations of interest and to study their behavior independently of the others peaks without changing the raw results.

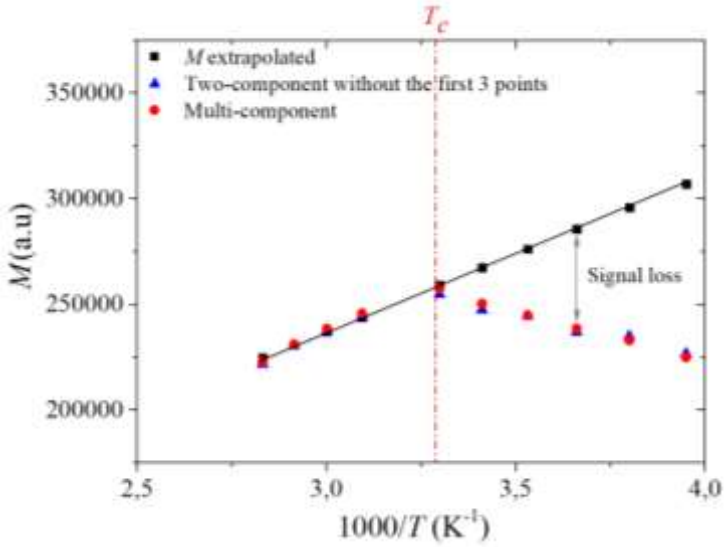

Figure SI-2. *First magnetization point measured in the case of a multi-components decomposition and 2 components decompositions after removing the 3 first points***.**

i) Distances between the confined liquid and the surfaces created during crystallization:

Assuming a single and uniform surface relaxivity, the ratios $[S/V]_{NMR}$ associated with the two different protons populations were determined by using equation (1) and $[S/V]_{SAXS}$ ratios obtained from SAXS measurements. The ratio $[V/S]_{NMR}$ is taken as a liquid distance between two crystals surfaces. The distance $d_1 = [V_1/S_1]_{NMR}$ for the main peak and $d_2 = [V_2/S_2]_{NMR}$ for the shoulder were calculated using the following equations:

$$\begin{cases} \dfrac{1}{T_{2(main\ peak)}} - \dfrac{1}{T_{2B}} = \rho_2 \left[\dfrac{S_1}{V_1}\right]_{NMR} = \mathrm{X}_1 \\ \dfrac{1}{T_{2\ (shoulder)}} - \dfrac{1}{T_{2B}} = \rho_2 \left[\dfrac{S_2}{V_2}\right]_{NMR} = \mathrm{X}_2 \end{cases} \quad \text{(SI.9)}$$

110

111 The limitation of this calculation method is that the proportion of protons contained in the
112 shoulder at high temperature (20 %) is taken into account at low temperatures which creates
113 uncertainties. The results obtained give only some orders of magnitude.

114 In first assumption, we took T_{2B} which corresponds to the unconfined liquid as the T_2
115 extrapolated from the main peak. Indeed, T_2 of the main peak, above T_c, followed a linear
116 behavior prolonged by the centrifuged oils before their WAT (**Figure SI-3**). Then, we get rid of
117 ρ_2 by dividing the two equations. By knowing that :

$$\begin{cases} \mathrm{S} = \mathrm{S}_1 + \mathrm{S}_2 \\ \mathrm{V} = \mathrm{V}_1 + \mathrm{V}_2 = \mathrm{a}_1\mathrm{V} + \mathrm{a}_2\mathrm{V} \end{cases} \quad \text{(SI.10)}$$

118 Where V corresponds to the total volume of liquid associated with the different proton
119 populations and a_1 and a_2 are respectively the main peak proportion and the shoulder proportion.
120 We established the relationship between $[S/V]_{RMN}$ to $[S/V]_{SAXS}$. The volume probed by NMR is
121 equal to the volume probed by SAXS weighted by the crystals volume fraction:

$$\left[\frac{S}{V}\right]_{RMN} = \left[\frac{S}{V}\right]_{SAXS} \times \frac{1}{(1-\phi)} = X3$$

122 Finally,

$$\begin{cases} \mathrm{d}_2 = \dfrac{a_2\left(1 + \dfrac{X_1}{X_2}\dfrac{a_1}{a_2}\right)}{X_3(1-\phi)} \\ \mathrm{d}_1 = \dfrac{a_1}{\left(\dfrac{X_1}{X_2}\dfrac{a_1}{a_2}\right)} \times \dfrac{d_2}{a_2} \end{cases} \quad \text{(SI.11)}$$

123

The results obtained for three temperatures are summarized in **Table SI.3** and show that $d_1 > 10d_2$. However, d_2 is of the same order of magnitude of as the size of a *n*-paraffin chain containing 15 carbons. Thus, the fast exchange model is not valid and the distances associated with each protons population cannot be determined by the present approach.

Table SI.3. *Liquid distances between surfaces estimated for the two protons population obtained from NMR/SAXS measurements at different temperatures.*

Temperature (°C)	T_{2B}	
	d_1 (nm)	d_2 (nm)
20	189	14.9
10	66	5.4
0	46	4.4

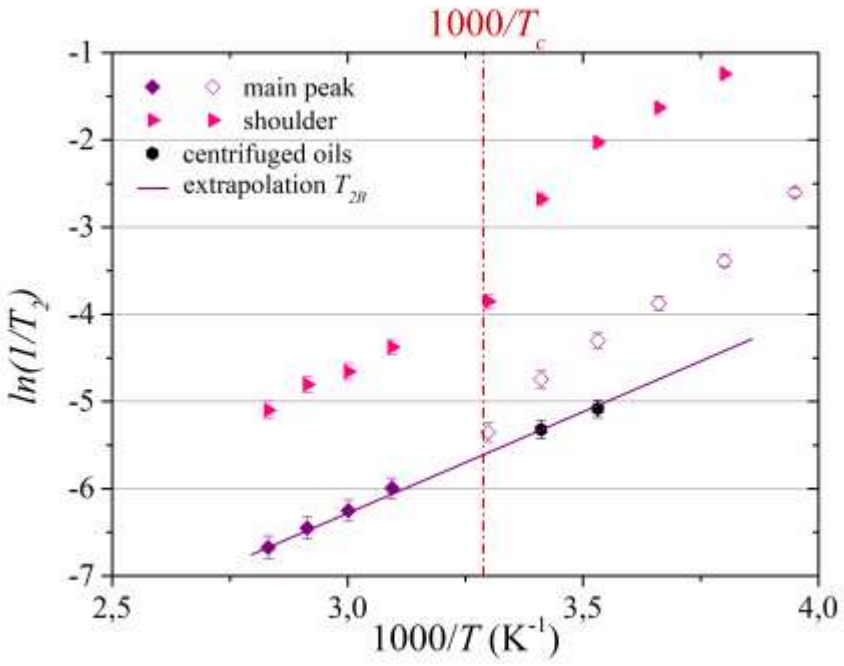

Figure SI-3 . *Evolution of the main peak and the shoulder relaxation rates, obtained from the 2 components distributions, versus the inverse of temperature for the crude oil.*